Contents lists available at ScienceDirect

Next Research

journal homepage: www.elsevier.com/locate/nexres

Biogenic synthesis of multifunctional copper oxide nanoparticles from *Coffea arabica* leaf extract for enhanced dye degradation and antimicrobial applications

Naveen Kumar Dabbeta [a], Mahesh Karne [a], Vijayalaxmi Katta [a], Sumana Yadagiri Konda [b], Anil Kumar Busi [c], Chittaranjan Rao Bandari [d], Ranga Ratan Kumar Palsapudi [a], Sreenivas Banne [e], Mika Sillanoää [f], Krishnakumar Balu [g], Parvathalu Kalakonda [a,*]

[a] *Smart Nano Materials Research Laboratory (SNRL), Department of Physics, Government City College (A), Osmania University, Hyderabad, 500002, India*
[b] *Department of Biochemistry, Government City College (A), Osmania University, Hyderabad, 500002, India*
[c] *Department of Chemistry, Government City College (A), Osmania University, Hyderabad, 500002, India*
[d] *Department of Zoology, Government City College (A), Osmania University, Hyderabad, 500002, India*
[e] *Center for Drug Discovery, Department of Pathology and Immunology, Government City College (A), Baylor College of Medicine, Houston, TX, 77030, USA*
[f] *Department of Civil Engineering, University Centre for Research & Development, Chandigarh University, Gharuan, Mohali, Punjab, India*
[g] *Department of Chemistry, Karpagam Academy of Higher Education (Deemed to be University), Coimbatore, 641021, Tamil Nadu, India*

ARTICLE INFO

Keywords:
CuONPs
Biosynthesis
Coffee leaf extract
Photocatalytic activity
Antibacterial activity

ABSTRACT

This work presents a novel and sustainable green synthesis route for copper oxide nanoparticles (CuONPs) using an aqueous extract of Coffea arabica leaves, an abundant and underutilized agro-waste product. The biosynthesized CuONPs exhibited a distinctive cuboid morphology, a feature uncommon in green synthesis along with a pure monoclinic crystal structure. SEM and XRD analyses showed that the particles were predominantly 100–300 nm in size, with crystallite sizes of 35–45 nm. FTIR spectroscopy confirmed the presence of phytochemical capping agents, while UV–Vis spectroscopy revealed characteristic absorption maxima at 283 nm and 330 nm, corresponding to an estimated optical energy bandgap of 2.75–2.85 eV. When subjected to visible-light illumination, the CuONPs demonstrated efficient dye removal, degrading 93 % of methylene blue (MB) and 87 % of rhodamine B (RhB) within 90 min, in a process following pseudo-first-order kinetic. Furthermore, antibacterial disk diffusion assay demonstrated pronounced inhibition of *Escherichia coli* (EPEC), underscoring the dual functional capacity of these biosynthesized nanoparticles. This approach transforms agro-waste into high-value, plasmonically active nanocatalysts, offering an environmentally responsible solution for simultaneous dye degradation and microbial disinfection in water treatment. The simple and inexpensive process is suitable for the large-scale production of versatile materials for environmental remediation.

1. Introduction

The unchecked discharge of toxic industrial effluents, particularly synthetic dyes from the textile sector, into aquatic ecosystems constitutes a critical global environmental and public health crisis [1,2]. The textile industry, a major contributor to this problem, is responsible for 20 % of global industrial water pollution largely due to inadequate treatment of dye-laden wastewater and insufficient waste management practices [3]. Methylene blue (MB) and rhodamine B (RhB) are commonly used dyes in multiple sectors such as textiles, paper manufacturing, cosmetics, and the pharmaceutical industry [4,5]. Once released into water bodies, they not only degrade water quality and disrupt photosynthetic activity by limiting light penetration but also bioaccumulate in aquatic organisms, leading to toxic effects that threaten biodiversity and human health. Addressing these complex and pressing issues demands innovative and sustainable solutions for the effectively remove dyes and associated pathogens from water bodies [6–11]. Recent advances have focused on developing metal nanocatalyst with dual photocatalytic and antibacterial properties, which enable the degradation of recalcitrant dyes and the elimination of harmful bacteria

* Corresponding author.
E-mail address: parvathalu@wpi.edu (P. Kalakonda).

https://doi.org/10.1016/j.nexres.2026.101508
Received 24 September 2025; Received in revised form 7 February 2026; Accepted 16 February 2026
Available online 17 February 2026

through visible-light-driven processes [12,13].

The photocatalytic degradation of dyes and the provision of bacteria-free water, utilizing noble metal catalysts and antibacterial agents, presents a sustainable solution for water purification [12,14]. This innovative process not only effectively removes pollutants from water bodies but also plays a crucial role in protecting aquatic life and supporting the overall health of ecosystems [6]. By facilitating the breakdown of harmful dyes and contaminants, photocatalysis contributes to cleaner water bodies, thereby supporting biodiversity and promoting environmental sustainability [6,12–23].

Metal nanomaterials (MNPs) have emerged as excellent supports for photocatalysts, primarily due to their significant charge storage capability, which helps reduce electron-hole recombination, and their high nanoscale surface-area to volume-ratio, which boosts catalytic efficacy [15,24]. Among various metal nanoparticles, CuONPs stand out for their superior photocatalytic and antibacterial properties. The enhanced properties can be attributed the relatively narrow band gap of CuONPs typically ranging from 1.76 to 3.5 eV, which enables efficient absorption of visible light [17,18,23–31]. As a result, CuONPs can produce reactive oxygen species (ROS) when exposed to light, a critical factor in the breakdown of various persistent organic pollutants. In addition, the broad optical absorption and effective separation of charge carriers in CuONPs further support their role as potent agents in environmental remediation [12,32,33]. Compared to other metal nanoparticles, these features make CuONPs particularly effective for applications requiring both high photocatalytic and antibacterial activity [16,20,34,35].

The use of leaf extracts for the green synthesis of metal nanoparticles has become an increasingly popular approach, offering a sustainable alternative to conventional chemical methods [22,28,29,31,20]. Coffee leaves are rich in antioxidants, flavonoids, and polyphenols-bioactive compounds that not only help reduce and stabilize metal ions during nanoparticle formation but also provide additional health benefits by combating oxidative stress and inflammation. These phytochemicals act as natural reducing agents, facilitating the formation of nanoparticles while simultaneously capping and stabilizing them, which enhances their functional properties and stability [36]. The abundance and diversity of such compounds in coffee leaves make them an attractive resource for developing novel metal-based catalysts. By utilizing these natural extracts, it is possible to produce nanomaterials that are both efficient and environmentally benign, aligning with the principles of green chemistry [37,38]. This methodology not only minimizes reliance on **hazardous** chemicals but also opens new avenues for the application of plant-derived nanomaterials in fields ranging from catalysis to biomedicine, ultimately supporting the development of innovative and sustainable technologies [27].

Although the use of plant extracts for the green synthesis of metal nanoparticles is widely recognized, there is an increasing demand to explore new, abundant, and cost-effective biological sources that can not only drive nanoparticle formation but also confer distinctive morphological and functional characteristics. Moreover, the creation of facilely synthesized, dual-functional nanomaterials capable of addressing both chemical and biological pollutants in tandem continues to pose a considerable challenge for researchers. Our research introduces an innovative approach to synthesizing CuONPs using coffee leaf extracts, a method that not only enhances the stability and morphology of the nanoparticles but also aligns with sustainable and green chemistry principles [17,25]. Unlike conventional chemical synthesis techniques, our biosynthetic route leverages natural phytochemicals, resulting in CuONPs with superior multifunctional properties, including remarkable optical, electrical, antibacterial, and photocatalytic characteristics [26,27,39]. A key highlight of our study is the first-time demonstration of the antibacterial activity and photocatalytic efficiency of coffee leaf-derived CuONPs for the degradation of MB and RhB water-soluble pollutants. This bio- synthesis method offers a dual benefit: it is environmentally benign and produces nanoparticles [40] that excel in antibacterial and water purification applications [41] through photocatalysis [13,17,20,42,43]. Furthermore, our CuONPs exhibit significant antibacterial activity, particularly against pathogenic strains such as *Escherichia coli* (*EPEC*), underscoring their potential for broader applications in water treatment and public health. The robustness, ease of recovery, and adaptability of these biosynthesized CuONPs make them highly suitable for integration into continuous industrial processes, including those in the environmental and biomedical sector [1,5,27,28,31,39,44,45,36]. Despite the inherent complexities in CuONP structure and active site identification, our method stands out for its scalability, cost-effectiveness, and minimal environmental impact. A significant challenge in sustainable nanotechnology is the creation of simple, multi-purpose materials from abundant, low-cost sources. While green synthesis methods have advanced, finding new biological resources that can produce nanoparticles with distinct shapes and properties remains a priority compared to other methods [11,16,18,23,36,33,46,47]. This study addresses this need by repurposing *Coffea arabica* leaf extract, an agricultural by-product, to fabricate cuboid-shaped copper oxide nanoparticles (CuO NPs). The research is novel in its pursuit of a dual-functional nanomaterial designed to combat both biological pathogens and chemical pollutants, such as synthetic dyes, in a single system.

In summary, our study not only pioneers the use of coffee leaf extracts for the green synthesis of highly effective CuONPs but also establishes their dual functionality in the degradation of MB and RhB pollutants and antimicrobial action. These findings position our eco-friendly CuONPs as a promising solution for sustainable environmental, biomedical, and advanced water purification applications.

2. Materials and methodology

2.1. Materials

Copper II nitrate ($Cu(NO3)_2{\cdot}3H_2O$) salts, acetone, toluene, and methylene blue (MB) and rhodamine B (RhB) dyes of high research grade were procured from Sigma-Aldrich, India, and were used without any further purification. Fresh coffee leaves were collected from a coffee garden in Andhra Pradesh, India.

2.2. Biosynthesis process of copper nanoparticles

Fresh coffee leaves were thoroughly washed, sun-dried, and ground into a fine powder. Two grams of the powdered leaves were steeped in 50 mL of deionized water at 75 °C for 30 min. After filtration, 40 mL of the resulting extract was slowly added to a 0.1 M $Cu(NO_3)_2$ $.3H_2O$ solution maintained at 80 °C with 500 rpm magnetic stirring. The reaction was allowed to proceed for 2 h at the natural pH of the mixture (the pH value was maintained at approximately 7 using NaOH pallets). The formation of CuONPs was indicated by a distinct color change from light blue to dark brown. The resulting precipitate was collected by centrifugation at 6000 rpm for 30 min, washed three times with deionized water and once with ethanol to remove any unreacted components, and then dried overnight at 60 °C. **To ensure complete oxidation, the dried powder was calcined in a muffle furnace at 300 °C for 2 h.** The final product was stored for further characterization and application. A schematic overview of the entire synthesis and testing protocol is presented in Fig. 1. All experiments, including photocatalytic degradation and antibacterial assays, were performed in triplicate ($n = 3$). The data are presented as the mean ± standard deviation.

2.3. Characterization of CuONPs

The synthesized CuONPs were characterized using several analytical techniques, as described in our previous work [21]. UV–Vis spectroscopy was used to confirm the formation of CuONPs by detecting surface plasmon resonance (SPR) absorption peaks. FTIR analysis identified functional groups from the plant extracts involved in reduction and

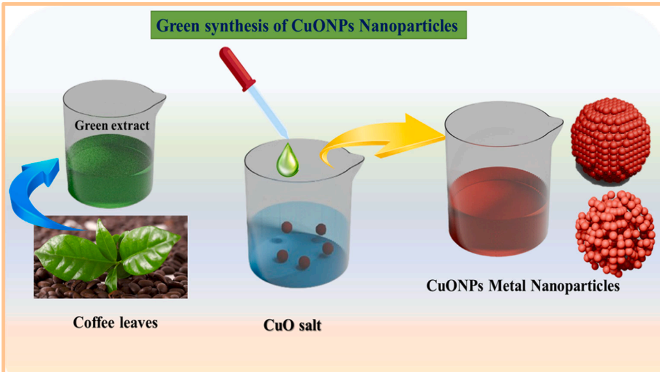

Fig. 1. Schematic diagram illustrating the green synthesis of CuONPs using *Coffea arabica* leaf extract.

stabilization of nanoparticle formation. SEM was used to examine the surface morphology, while XRD confirmed the crystal structure and phase of the CuONPs. Together, these techniques provided comprehensive analysis of the catalyst and their functional properties.

2.4. Antibacterial activity assay

The antibacterial activity of the CuONPs was assessed using the disc diffusion assay against the Gram-negative bacterium EPEC. A 30 µg dose of CuONPs was incubated with 10^7 CFU of EPEC in 100 µl of LB medium at 37 °C for 6 h. An Untreated EPEC culture was used as a negative control. Bacterial growth was estimated by measuring optical density (OD) at 600 nm before and after incubation. The diameter of the inhibition zone was measured in millimeters to quantify the antibacterial effectiveness of the CuONPs.

2.5. Photocatalytic activity & dye degradation process

CuONPs demonstrated strong photocatalytic performance in the dye degrading MB & RhB dyes when exposed to visible light. The 10 W LED light source (equipped with a 420 nm cut-off filter, light intensity: 8000 Lux, distance: 15 cm) have been used to test photocatalytic activity. UV–Vis spectroscopy revealed a gradual reduction in the absorption at 668 nm as the irradiation time increased. Over the 90-minute period, the intensity of the MB and RhB peaks significantly decreased, indicating substantial MB & RhB dye degradation. The calculated degradation percentage confirmed that CuONPs significantly accelerated the breakdown of MB & RhB dye under the experimental conditions [39].

$$Degradation(\%) = \left(\frac{C_0 - C_t}{C_0}\right) \times 100$$

Here, C_0 indicates the absorption at time $t = 0$, C_t indicates the absorption at the end of time t.

3. Results and discussion

3.1. Scanning electron microscopy (SEM)

Scanning electron microscopy (SEM) images presented in Fig. 2 reveal the morphological characteristics of the CuONPs, displaying a distinctive cuboid shape with an average particle size of 135±5 nm. The CuONPs were also observed to be uniformly dispersed and arranged in a densely packed structure. The unique morphology, characterized by a smooth surface and diverse particle sizes, suggests effective stabilization by bioactive compounds present in the coffee leaf extract. These stabilizing agents likely play a crucial role in enhancing the catalytic and antibacterial performance of the CuONPs. Variations in particle shape and size are most likely due to differences in nucleation and growth dynamics during the synthesis process. The discrepancy between the average CuONPs nanoparticle size from SEM micrographs (~135 nm) and the crystallite size from XRD analysis (35–45 nm) indicates that the cuboid particles are polycrystalline aggregates composed of multiple smaller crystallites.

3.2. Fourier transform infrared spectroscopy (FTIR)

The Fourier-transform infrared (FTIR) spectrum of the synthesized copper oxide nanoparticles showed a pronounced absorption band close to 650 cm^{-1}, which is indicative of **Cu–O** bond formation and confirms the creation of copper oxide at the nanoscale. A broad absorption feature observed near 3350 cm^{-1} corresponds to the stretching vibrations of hydroxyl (**O–H**) groups present on the nanoparticle surface. The peaks in the 1350–1650 cm^{-1} range, specifically at ~1630 cm^{-1} and ~1390 cm^{-1}, are characteristic of amide groups from proteins and carboxylate groups from polyphenols present in the coffee leaf extract [48,49]. These biomolecules are instrumental in reducing Cu^{2+} ions and capping the formed CuONPs, contributing to their stability and unique cuboid morphology. The identification of these functional groups supports the structural characterization of the nanoparticles and implies that plant-derived biomolecules serve as capping agents, which may improve both the stability and catalytic activity of the CuONPs. Fig. 3 displays the FTIR analysis results for the prepared CuONPs.

3.3. UV–VIS spectroscopy

The absorption occurred in the 270–380 nm range, with distinct peaks observed at 283 nm and 330 nm, which are consistent with reported values of CuO nanoparticles (Fig. 4) corresponding to electronic transitions within the nanostructures [31,31]. This pronounced

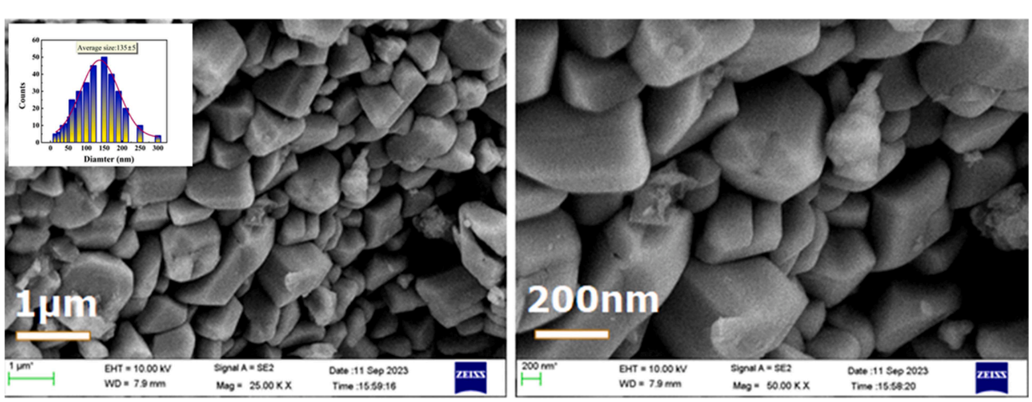

Fig. 2. SEM micrographs of CuONPs synthesized via a green method using coffee leaf extract. The inset shows the particle size distribution histogram, indicating an average particle size of ~135 ± 5 nm (accelerating voltage of 15 kV and high vacuum mode).

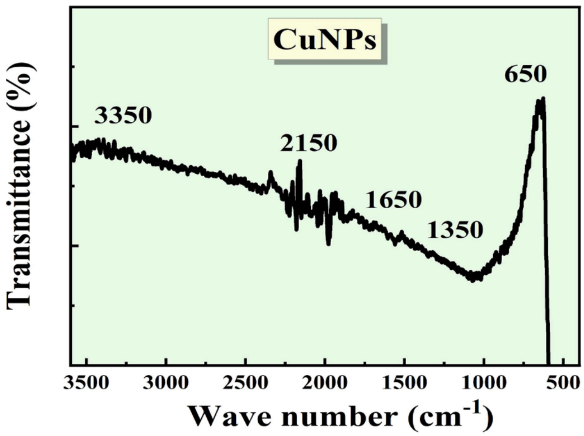

Fig. 3. FTIR spectrum of biosynthesized CuONPs, confirming the presence of phytochemical functional groups from the *Coffea arabica* leaf extract acting as capping and stabilizing agents.

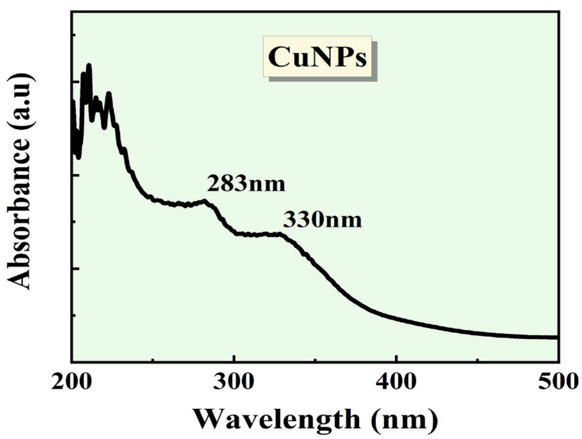

Fig. 4. UV–Vis absorption spectrum confirming the synthesis of CuONPs, showing a characteristic absorption peak in the UV region due to surface plasmon resonance.

ultraviolet absorption not only confirmed the successful synthesis of CuONPs but also indicated their nanoscale size, as evidenced by quantum confinement effects. As the wavelength approached the visible region, a gradual decline in absorbance was noted, suggesting that the synthesized CuONPs have a relatively wide band gap and display minimal absorption in the visible range, which aligns with typical semiconductor behavior. A broad shoulder observed in the absorbance spectrum was attributed to plasmonic effects and higher-order electronic transitions of Cu^{2+} ions, likely stabilized by phytochemicals from the coffee leaf extract used in the synthesis process. The presence of a wide band gap in these CuONPs supports their effectiveness as photocatalysts under ultraviolet irradiation and contributes to their distinctive optical behavior at the nanoscale. Bioactive constituents in the coffee extract, including polyphenols, flavonoids, and various antioxidants, not only aided in reducing copper ions to form CuONPs but also contributed to nanoparticle stabilization, ultimately shaping their UV–Vis absorption profile.

The optical band gap energies of the CuONPs were determined using UV–Vis Tauc plot analysis ($(\alpha h\nu)^n$ vs. $h\nu$), yielding values of 2.75 eV for direct electronic transitions and 2.85 eV for indirect transitions, as illustrated in Fig. 5 (A & B). These band gap values are higher than those reported for bulk copper oxides (approximately 1.2–2.2 eV), a difference attributed to quantum confinement effects arising from the nanoscale dimensions of the CuONPs, which produce discrete energy levels instead of continuous bands [50,49]. The Tauc plots were analyzed for both direct and indirect transitions to assess the optical behavior. The stronger linear fit for the direct transition plot suggests that the CuONPs exhibit predominant direct band gap transitions. The linear region observed in the Tauc plot indicates that the CuONPs possess direct band gap characteristics, allowing electrons to transition from the valence band to the conduction band without the need for phonon involvement. The measured direct (2.75 eV) band gaps highlight the distinctive optical properties of the green-synthesized CuONPs, setting them apart from copper oxides produced by conventional methods, which typically exhibit bulk-like band gaps. The combination of improved optical characteristics and environmentally friendly biosynthesis underscores the promise of these CuONPs for use in environmental remediation and antibacterial water purification technologies.

3.4. X-Ray diffraction (XRD)

X-ray diffraction (XRD) analysis of the CuONPs produced with coffee leaf extract revealed a distinct crystalline structure, as illustrated in

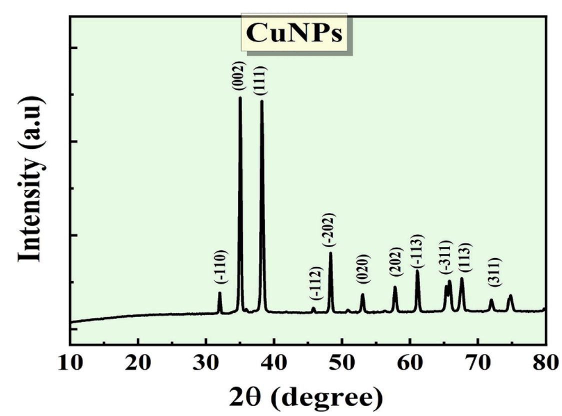

Fig. 6. XRD pattern of the biosynthesized CuONPs, confirming a monoclinic crystal structure matched to the reference pattern for CuO (JCPDS 01–0866–8837).

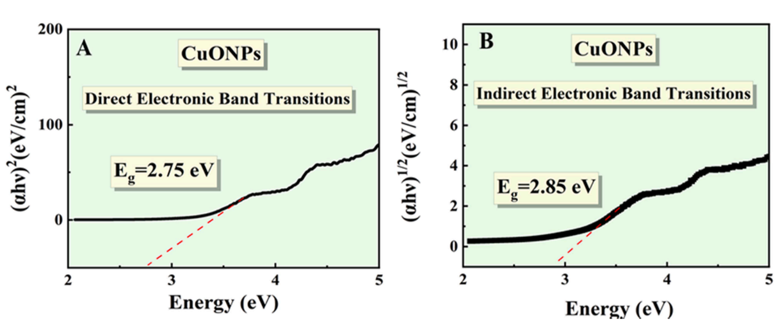

Fig. 5. Tauc plots showing the (A) direct (2.75 eV) and (B) indirect (2.85 eV) optical band gaps of the CuONPs, as calculated from UV–Vis absorption data.

Fig. 6. The analysis showed distinct diffraction peaks at specific 2θ angles: 32.5° (−110), 35.5° (002), 38.7° (111), 48.8° (−202), 53.6° (020), 58.3° (202), 61.5° (−113), 66.0° (311), 72.2° (−313), and 74.6° (311) [29]. These reflections matched the standard pattern for monoclinic copper oxide, as referenced by JCPDS card number 01–0866–8837, confirming the successful green synthesis and crystallinity of the nanoparticles. The pronounced sharpness and intensity of these peaks further emphasized the nanoscale features of the synthesized CuONPs. The average crystallite size of the CuONPs was estimated using the Debye-Scherrer equation, which is expressed as $D = 0.9\lambda/\beta\cos\theta$, where D is the crystallite size, k is a constant typically taken as 0.9, λ is the wavelength, β is the full width at half maximum (FWHM) of the peak in radians, and θ is the Bragg angle corresponding to the maximum intensity peak position. The crystallite sizes of the CuONPs were found to range between **35 and 45 nm**. The lack of extraneous peaks in the XRD pattern indicated the high purity of the synthesized nanoparticles, highlighting their suitability for applications in bionanotechnology and advanced materials research.

Table 1 presents the specific diffraction angles along with the corresponding crystallite sizes of the synthesized copper oxide nanoparticles (CuONPs). Additionally, the lattice constants were calculated using Bragg's law, providing further insight into the crystalline structure of the nanoparticles. The formation mechanism of CuONPs using coffee leaf extract is thought to involve both oxidation reactions and electrostatic interactions. A noticeable color change was observed within 20 to 30 min of synthesis, indicating that oxidation plays a central role in the formation of CuONPs. Electrostatic stabilization further contributed to controlling the nucleation and growth of the nanoparticles. Employing plant extracts as green reducing and stabilizing agents offers a cost-effective, non-toxic, and environmentally sustainable approach, supporting the scalable production of CuONPs and other nanomaterials.

3.6. Antibacterial activity-disc diffusion

Enteropathogenic *E. coli* (*EPEC*) is recognized as a leading cause of persistent diarrhea globally, representing a serious public health issue. The antibacterial activity of copper oxide nanoparticles (CuONPs) synthesized from coffee leaf extract against *EPEC* was evaluated using a disc diffusion assay, as illustrated in Fig. 7. The disc loading concentration (30 µg/disc) was used and a distinct zone of inhibition formed around the CuONPs disc. A clear zone of inhibition with an average diameter of 10 mm was observed, demonstrating pronounced antibacterial effects against EPEC. A gentamicin disc (10 µg/disc) was used as a positive control, showing a zone of inhibition of 22 mm. In contrast, no inhibition zones were observed around the CL extract, PBS, or untreated *EPEC* discs, confirming that the CuONPs were solely responsible for suppressed bacterial growth. This antibacterial activity is likely mediated by the release of Cu^{2+} ions and the generation of reactive oxygen species, which cause damage to the bacterial cell envelope and internal components.

3.7. Photo-catalytic activity of CuONPs

Fig. 8(A) and (B) demonstrate the photocatalytic activity of the CuONPs in degrading MB and RhB dyes at a concentration of 50 ppm. The rate of dye degradation depended on several parameters, including exposure time, light intensity, initial dye concentration, and catalyst dosage. In this work, a **10 W LED** bulb served as the illumination source. A total of **3 mg** of the CuONPs catalyst was added to the dye solution, which was the stirred and kept in the dark for 5 min to reach **adsorption–desorption equilibrium**. Afterward, the mixture was subsequently exposed to **10 W** LED light, and aliquots were withdrawn at specific intervals to monitor the absorbance using UV–Vis spectroscopy.

Table 1
Crystallographic parameters of green-synthesized CuONPs derived from XRD analysis, including peak position (2θ) and calculated crystallite size.

S.NO	2θ(CuONPs)	Crystalline size (nm)
1	35	21.9
2	38.2	44.1
3	48.3	44.5
4	50.87	46.1
5	61.13	46.5
6	67.7	45.5
7	74.7	34.4

The UV–Vis spectra showed a significant reduction in absorbance at 661 nm, indicating an effective degradation of the MB dye. Initially, the absorbance peak was at its highest absorption but decreased markedly, reaching almost zero within 90 min of light exposure. RhB dye is a more complex molecules with a carboxylate group, making it potentially more recalcitrant than the smaller, planar thiazine dye MB. As summarized in Table 2, the photocatalytic efficiency of our coffee-leaf-derived CuONPs is competitive with, and in some cases superior to, other green-synthesized CuO nanomaterials reported in recent literature, particularly considering the relatively short degradation time of 90 min. These results highlight the catalyst efficiency of CuONPs , which was likely due to their large surface area, nanoscale size, and well-defined crystalline structure. These characteristics enhanced electron transfer and promoted the formation of reactive oxygen species (ROS), which accelerated the breakdown of MB dye molecules. The consistent decrease in absorbance underscores the potential these CuONPs for applications in wastewater treatment and remediation of organic pollutants, providing a sustainable approach to addressing environmental challenges.

A direct comparison of degradation efficiencies across studies is limited by differences in experimental conditions such as light source, catalyst loading, and dye concentration. Despite these variables, our coffee-leaf-derived CuONPs show competitive performance under moderate visible-light conditions, which we attribute to their unique morphology, crystallinity, and phytochemical capping. This highlights their potential as effective, green-synthesized photocatalysts.

Fig. 9 (A & B) illustrates the photocatalytic degradation of methylene blue (MB) and rhodamine B (RhB) dyes, each at an initial concentration of 50 ppm, using 3 mg of CuONPs as the catalyst. Over a 90-minute reaction period, a marked reduction of its absorbance reaching near to zero and underscoring the high catalytic efficiency of the CuONPs. At the start of the experiment, the absorbance values were at their highest, corresponding to the initial concentrations of MB and RhB. As the photocatalytic reaction proceeded, the absorbance values steadily declined, indicating efficient degradation of both dye molecules. By the end of the 90-minute period, the absorbance had reached its lowest levels, highlighting the superior catalytic performance of the CuONPs. The observed difference in degradation efficiency between MB (93 %) and RhB (87 %) can be attributed to the distinct molecular structures and degradation pathways of the two dyes. The smaller size and simpler structure of MB likely facilitate easier adsorption onto the catalyst surface and subsequent radical-based breakdown compared to the more complex RhB molecule. The lower degradation efficiency for RhB (87 %) compared to MB (93 %) can be attributed to its more complex molecular structure and a carboxylate group, which enhance its stability and resistance to oxidative degradation. The remarkable photocatalytic activity can be attributed to the high surface area and crystallinity of the CuONPs, which enhance the degradation process. These findings underscore the promise of CuONPs as effective catalysts for wastewater treatment applications.

Initially, the absorbance readings were at their maximum, reflecting the starting concentrations of methylene blue (MB) and rhodamine B (RhB). The degradation of MB and RhB was primarily driven by the generation of reactive oxygen species and hydroxyl radicals, which attacked and decomposed the dye molecules. As light exposure continued, the color intensity of both dye solutions progressively diminished, signifying ongoing photocatalytic degradation. At an initial concentration of 50 ppm, the degradation efficiency reached

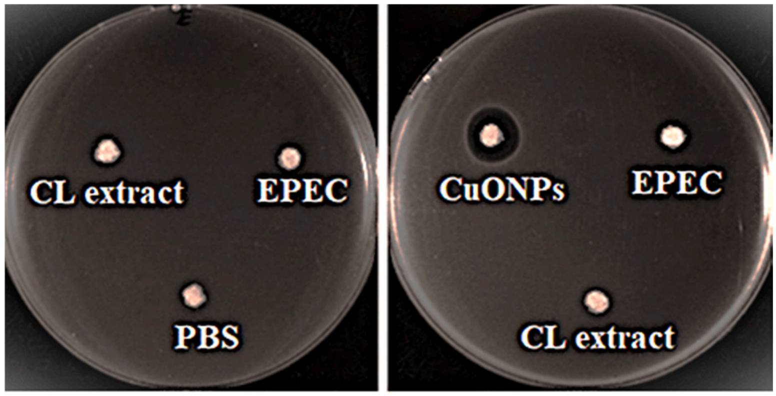

Fig. 7. Antibacterial activity of biosynthesized CuONPs against enteropathogenic *E. coli* (EPEC), evaluated using a disc diffusion assay.

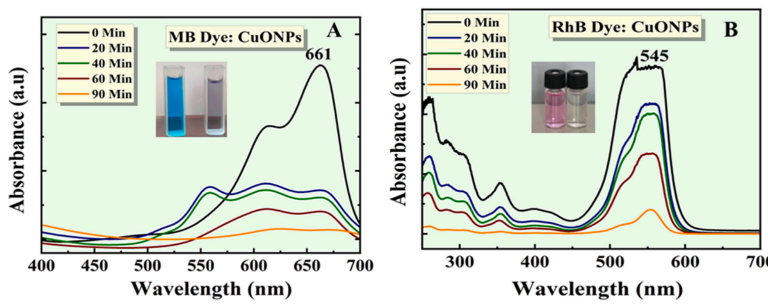

Fig. 8. Photocatalytic degradation of (A) methylene blue (MB) and (B) rhodamine B (RhB) dyes using coffee-leaf-synthesized CuONPs.

Table 2
Comparative analysis of dye degradation efficiency: The performance of coffee-leaf-synthesized CuONPs (this work) versus other green-synthesized catalysts.

Plant exatract	Nanoparticle	Target Pollutant	Degradation (%) / Time	Reference
Coffea arabica leaf (This work)	CuO	Methylene Blue (MB)	93 % / 90 min	This work
Coffea arabica leaf (This work)	CuO	Rhodamine B (RhB)	87 % / 90 min	This work
Durian Husk	CuO	Methyl Orange	91 % / 120 min	[23,51]
Garcinia mangostana leaf	CuO	POME	~85 % / 150 min	[50]
Muntingia calabura leaf	CuO	Rhodamine B	95 % / 180 min	[30]
Papaya Peel	CuO	Methylene Blue	89 % / 100 min	[28]

approximately 93 % for MB and 87 % for RhB, as shown in Fig. 10 (A and B). These findings highlight the remarkable photocatalytic performance of the catalyst and provide valuable insights for developing efficient dye removal technologies for industrial wastewater treatment.

3.8. Kinetic studies of CuONPs catalyst

The photocatalytic degradation of MB and RhB dyes using CuONPs was analyzed with the first-order kinetic model, where the rate of degradation was proportional to dye concentration at any time. Mathematically, this model was expressed [46] as $\ln\left(\frac{C_0}{C_t}\right) = kt$ here, C_o concentration at begging of process and C_t concentration at a given time t.

Fig. 11 (A and B) shows the kinetic plots for the degradation of MB and RhB dyes using green-synthesized CuONPs, which were analyzed using a first-order kinetic theory model. The plot between $\ln(C_0/C)$ versus time produces a straight line, indicating that the reaction follows first-order kinetics. The slope of the line, 0.027min^{-1}, and 0.030 min^{-1} represented the reaction rate constant (k), and provided a measure of the effectiveness of the CuONPs in promoting the dye degradation. An R-squared value of 0.94 demonstrated a strong linear correlation, confirming the reliability of the first-order kinetic model. This analysis highlighted the catalytic potential of bio-synthesized CuONPs for

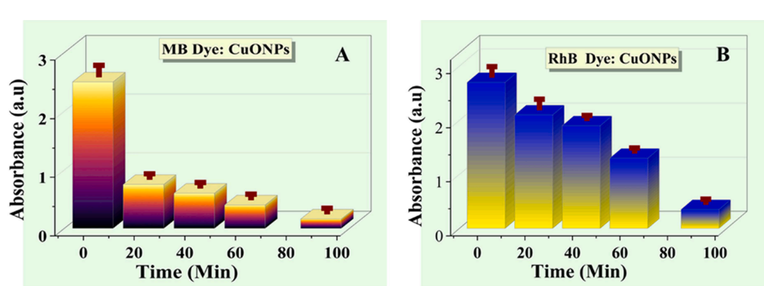

Fig. 9. Time-dependent UV–Vis absorption spectra for the photocatalytic degradation of (A) methylene blue (MB) and (B) rhodamine B (RhB) using 3 mg of CuONPs.

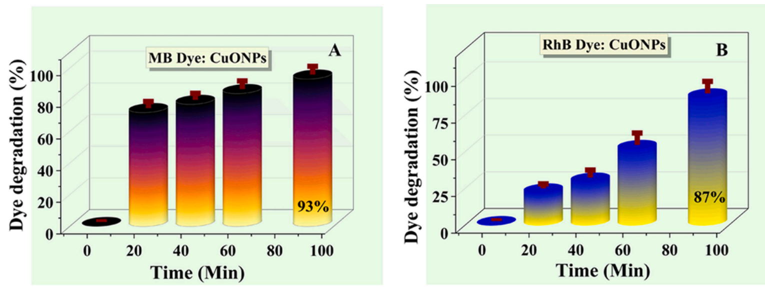

Fig. 10. Photocatalytic degradation percentage of (A) methylene blue (MB) and (B) rhodamine B (RhB) dyes using 3 mg of CuONPs.

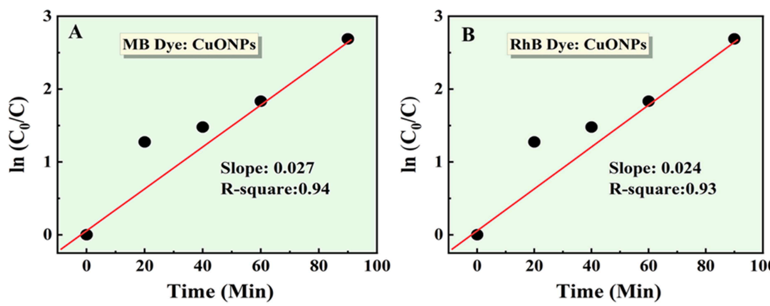

Fig. 11. Pseudo-first-order kinetic plots ($\ln(C_0/C)$ vs. time) for the photocatalytic degradation of (A) methylene blue (MB) and (B) rhodamine B (RhB) dyes using CuONPs.

environmental applications.

Fig. 12 (A and B) shows the degradation kinetics of MB and RhB dyes using CuONPs catalyst, showing the normalized concentration ratio (C/C_0) plotted against time. The curve showed a gradual decline in the dye concentration over time, indicating the catalytic activity of the CuONPs in degrading MB and RhB. The downward trend follows first-order kinetic behavior, as evidenced by the exponential decay-like profile of the plot. This analysis highlighted the effectiveness of CuONPs as a green catalyst for removal of a wide range of pollutants.

3.9. Possible mechanism of CuONPs catalyst

Photocatalytic detoxification of MB and RhB dyes present several challenges, especially under light irradiation [52]. The mechanism, illustrated in Fig. 13, utilizes CuONPs as the catalyst. Due to their narrow band gap, these NPs efficiently generate electron-hole pairs with reduced recombination, requiring less energy for electron transitions [53]. Upon exposure to light, CuONPs absorbed photons with matching their band gap, rapidly initiating the photocatalytic degradation of the dye. The fundamental catalytic process is shown below.

$$Photcatalyst\ CuONPs + h\nu \rightarrow e^- + h^+$$

$$Photcatalyst\ CuONPs\ (e^-) + h\nu \rightarrow O_2^-$$

$$Photcatalyst\ CuONPs\ (h^+) \rightarrow H_2O - OH^-$$

$$O_2^-\ (or) OH^- + MB/Rd\ dyes \rightarrow Degraded\ manterial$$

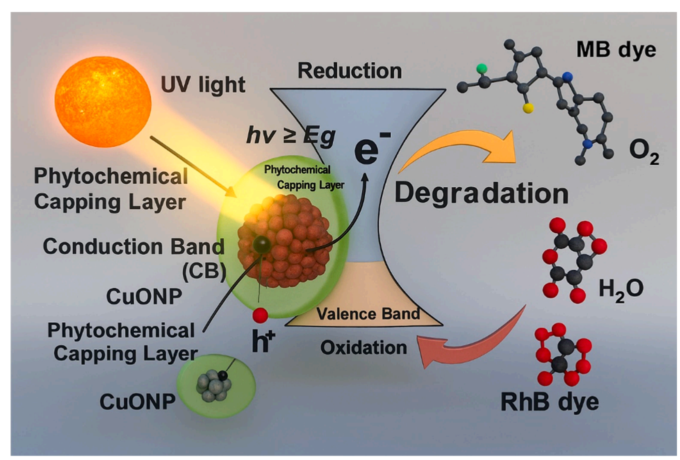

Fig. 13. Schematic illustration of the proposed photocatalytic mechanism for CuONPs, showing the generation of reactive oxygen species (ROS) under light irradiation leading to dye degradation.

During photocatalysis, electron excitation from the valence band to the conduction band creates electron-hole pairs. The holes (h^+) in the

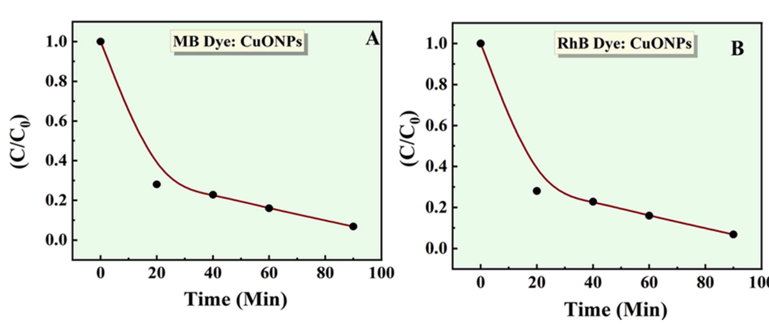

Fig. 12. First-order kinetic analysis for the degradation of (A) MB and (B) RhB dyes catalyzed by CuONPs, showing the plot of C/C_0 versus time.

valence band acting as electron acceptors from pollutant molecules, thereby initiating dye breakdown. This process generated reactive species: water molecules convert into hydroxyl radicals ($^{\bullet}OH$), and oxygen molecules react with conduction band electrons to form superoxide radicals ($^{\bullet}O_2^-$), both of which play a crucial role in degrading organic contaminants [54]. The high catalytic activity of CuONPs is attributed to their rapid charge carrier release and enhanced electron delocalization, which contributes to NPs stabilization. Additionally, phenolic and bioactive compounds from coffee leaf extract adsorbed onto the CuONPs surface, further promote superoxide radical generation, resulting in increased photocatalytic efficiency. Our findings demonstrated that hydroxyl and super oxide radicals were central to the degradation of water-soluble MB and RhB dyes, supporting the use of the CuONPs as an effectiveness and sustainability of CuONPs as catalysts for environmental remediation. The phytochemical capping layer from coffee leaf extract not only stabilizes the CuONPs but also facilitates electron transfer, acting as a sensitizer under visible light. This enhances charge separation and promotes the generation of reactive oxygen species (ROS), thereby improving photocatalytic efficiency.

4. Conclusion

This study pioneers a facile and eco-friendly synthesis of multifunctional copper oxide nanoparticles (CuONPs) using *Coffea arabica* leaf extract, a renewable agro-waste material. The phytochemical profile of the extract directly influenced the formation of CuONPs with a unique cuboid morphology, a monoclinic crystal structure, and bio-derived surface functional groups that enhance their stability and reactivity. Thorough characterization confirmed these attributes, including a distinct optical bandgap (2.75–2.85 eV) conducive to visible-light photocatalysis. The biosynthesized CuONPs demonstrated exceptional dual-functionality: they achieved rapid degradation of methylene blue (93 %) and rhodamine B (87 %) within 90 min under visible light, with performance comparable or superior to conventional catalysts, as confirmed by pseudo-first-order kinetics. Furthermore, the nanoparticles exhibited potent antibacterial activity against pathogenic *E. coli* (EPEC). This effective combination of superior dye degradation and significant antibacterial efficacy positions coffee-leaf-derived CuONPs as a highly promising, sustainable, and cost-effective nanocatalyst for next-generation water purification technologies. Future work will focus on evaluating the reusability of the CuONPs over multiple cycles, assessing their ecotoxicity, and validating their efficacy with real industrial wastewater samples to determine practical applicability.

Declaration

Parvathalu Kalakaonda (PK): Project designing, visualization of the project and discussion mechanism, and draft writing.

Naveen Kumar Debbeta, Mahesh Karne, Ranga Ratan Kumar Palsapudi, Vijayalaxmi Katta: Designing various experiments, data collection & analysis, and project completion

Sumana Yadagiri Konda, Anil Kumar Busi, Chittaranjan Rao Bandari, Sreenivas Banne, Krishnakumar Balu: proof reading and discussion of the project.

Ethical approval

The institute board committee of our lab stated that we do not have any consent to publish this work.

CRediT authorship contribution statement

Naveen Kumar Dabbeta: Data curation. **Mahesh Karne:** Data curation. **Vijayalaxmi Katta:** Methodology, Data curation. **Sumana Yadagiri Konda:** Data curation. **Anil Kumar Busi:** Data curation. **Chittaranjan Rao Bandari:** Data curation. **Ranga Ratan Kumar Palsapudi:** Data curation. **Sreenivas Banne:** Writing – review & editing, Data curation. **Mika Sillanoää:** Writing – review & editing. **Krishnakumar Balu:** Writing – review & editing. **Parvathalu Kalakonda:** Writing – review & editing, Writing – original draft, Visualization, Supervision, Formal analysis.

Declaration of competing interest

The authors declare that they have no known competing financial interests or personal relationships that could have appeared to influence the work reported in this paper.

Acknowledgements

The authors extend thanks to Smart Nano material Research Laboratory (SNRL), Dept. of Physics, Government City College (A); Osmania University for supporting basic facilities and characterization of materials.

No funding was received for this project.

References

[1] T. Rajaram, A. Das, Water pollution by industrial effluents in India: discharge scenarios and case for participatory ecosystem specific local regulation, Futures 40 (1) (2008) 56–69, https://doi.org/10.1016/j.futures.2007.06.002.

[2] L. Gupta, M. Bansal, P. Nandi, G. Habib, R. Sunder Raman, Source apportionment and potential Source regions of size-resolved particulate matter at a heavily polluted industrial City in the Indo-Gangetic plain, Atmos. Environ. 298 (2023) 119614, https://doi.org/10.1016/j.atmosenv.2023.119614.

[3] K.G. Pavithra, Removal of colorants from wastewater: a review on sources and treatment strategies, J. Ind. Eng. Chem. 75 (2019) 1–19, https://doi.org/10.1016/j.jiec.2019.02.011.

[4] I. Khan, K. Saeed, I. Zekker, B. Zhang, A.H. Hendi, A. Ahmad, S. Ahmad, N. Zada, H. Ahmad, L.A. Shah, T. Shah, I. Khan, Review on Methylene blue: its properties, uses, toxicity and photodegradation, Water (Basel) 14 (2) (2022) 242, https://doi.org/10.3390/w14020242.

[5] R.H. Waghchaure, V.A. Adole, B.S. Jagdale, Photocatalytic degradation of methylene blue, rhodamine B, methyl orange and eriochrome black T dyes by modified ZnO nanocatalysts: a concise review, Inorg. Chem. Commun. 143 (2022) 109764, https://doi.org/10.1016/j.inoche.2022.109764.

[6] A. M. Ismail, K. Akhtar, M.I. Khan, T. Kamal, M.A. Khan, M. Asiri, J. Seo, S.B Khan, Pollution, toxicity and carcinogenicity of organic dyes and their catalytic bio-remediation CPD 25 (34) (2019) 3645–3663, https://doi.org/10.2174/1381612825666191021142026.

[7] T. Islam, Md.R. Repon, T. Islam, Z. Sarwar, M.M. Rahman, Impact of textile dyes on health and ecosystem: a review of structure, causes, and potential solutions, Environ. Sci. Pollut. Res. 30 (4) (2022) 9207–9242, https://doi.org/10.1007/s11356-022-24398-3.

[8] U. Shanker, M. Rani, V. Jassal, Degradation of hazardous organic dyes in water by nanomaterials, Environ. Chem. Lett. 15 (4) (2017) 623–642, https://doi.org/10.1007/s10311-017-0650-2.

[9] M.L. Sall, A.K.D. Diaw, D. Gningue-Sall, S. Efremova Aaron, J.-J. Aaron, Toxic heavy metals: impact on the environment and Human health, and treatment with conducting organic polymers, a review, Environ. Sci. Pollut. Res. 27 (24) (2020) 29927–29942, https://doi.org/10.1007/s11356-020-09354-3.

[10] M. Shabir, M. Yasin, M. Hussain, I. Shafiq, P. Akhter, A.-S. Nizami, B.-H. Jeon, Y.-K. Park, A review on recent advances in the treatment of dye-polluted wastewater, J. Ind. Eng. Chem. 112 (2022) 1–19, https://doi.org/10.1016/j.jiec.2022.05.013.

[11] M. Ebrahimi, N. Khalili, S. Razi, M. Keshavarz-Fathi, N. Khalili, N. Rezaei, Effects of lead and cadmium on the immune system and cancer progression, J. Environ. Health Sci. Eng. 18 (1) (2020) 335–343, https://doi.org/10.1007/s40201-020-00455-2.

[12] I. Hasan, A. Bassi, P. Kalakonda, K. Kanungo, ZnO-doped Kaolin Nanoclay immobilized Agar biopolymer for 2,4-dinitrophenol photocatalytic degradation, Asia-Pac. J. Chem. Eng. 19 (6) (2024) e3144, https://doi.org/10.1002/apj.3144.

[13] A. Bassi, P. Kalakonda, I. Hasan, Synthesis of Chitosan-Agar immobilized NiO-MgO bionanocomposites and their photocatalytic application towards toxic azo dye, Inorg. Chem. Commun. 170 (2024) 113499, https://doi.org/10.1016/j.inoche.2024.113499.

[14] P. Kalakonda, A. Bashitangu, P. Mandal, S. Jowhar Khanam, M. Banovath, I. Hasan, B. Bhaskar Podila, Sustainable Solutions for clean water: green synthesized Cu-Ag-bimetallic nanoparticles based nano catalyst, Mater. Sci. Eng.: B 301 (2024) 117147, https://doi.org/10.1016/j.mseb.2023.117147.

[15] U. Qumar, J.Z. Hassan, R.A. Bhatti, A. Raza, G. Nazir, W. Nabgan, M. Ikram, Photocatalysis vs adsorption by metal oxide nanoparticles, J. Mater. Sci. Technol. 131 (2022) 122–166, https://doi.org/10.1016/j.jmst.2022.05.020.

[16] Y.B. Chan, M. Aminuzzaman, Y.F. Win, S. Djearamane, L.S. Wong, S.K. Guha, H. Almohammadi, Md. Akhtaruzzaman, L.-H. Tey, L. Garcinia Mangostana, Leaf-

extract-assisted green synthesis of CuO, ZnO and CuO-ZnO nanomaterials for the photocatalytic degradation of palm oil mill effluent (POME), Catalysts 14 (8) (2024) 486, https://doi.org/10.3390/catal14080486.

[17] R. Chowdhury, A. Khan, Md.H. Rashid, Green synthesis of CuO nanoparticles using *Lantana Camara* flower extract and their potential catalytic activity towards the Aza-Michael reaction, RSC Adv. 10 (24) (2020) 14374–14385, https://doi.org/10.1039/D0RA01479F.

[18] N.K. Dabbeta, M. Kante, R. Konda, A. Devarala, P.B. Kalakonda, S.J. Khanam, R. N. Savu, M. Banovath, L.S.R. Siddey, V.N. Bommaji, I. Hasan, P. Kalakonda, Eco-inspired Cu-Zn bimetallic nanoparticles for enhanced water purification technologies, Mater. Chem. Phys.: Sustain. Energy 2 (2025) 100013, https://doi.org/10.1016/j.macse.2025.100013.

[19] C. Hou, J. Zhao, L. Yang, J. Chen, X. Xia, X. Zhou, Y. Zhang, A single-atom Fe-N-C catalyst with superior fenton-like reaction performance prepared facilely using microalgae: key roles of oxygen and interactions between Fe-nx and Fe/Fe compounds, Appl. Catal. B: Environ. 339 (2023) 123135, https://doi.org/10.1016/j.apcatb.2023.123135.

[20] P. Kalakonda, M. Thodeti, C. Ganneboina, K. Ankathi, S. Kathri, K. Begari, H. S. Kante, V. Jupalli, Y. Khaderabad, S. Vijaylaxmi, V. Morampudi, P. Mandal, V. R. Yatham, I. Hasan, B.B. Podila, Eco-friendly fabrication of silver nanoparticles for sustainable water purification and antibacterial synergy, Plasmonics 19 (6) (2024) 2857–2869, https://doi.org/10.1007/s11468-024-02251-2.

[21] S.C.Y. Lim, M.X. Koh, Y.B. Chan, S. Djearamane, C.-S. Yeh, C.-H. Chen, L.S. Wong, L.-H. Tey, Green synthesis of cr_2o_3-MCC microcomposite for photocatalytic degradation of Congo red, crystal violet, and methylene blue in wastewater treatment, J. Taiwan Inst. Chem. Eng. (2025) 106368, https://doi.org/10.1016/j.jtice.2025.106368.

[22] V. Mariyappillai, C. Shiyamala, M. Tiffany, T. Abisheik, V. Pandiyan, A.K. Alanazi, P. Kalakonda, A. Thirumurugan, G. Sandoval-Hevia, K. Balu, A sustainable approach to water purification: strontium-modified ZnO nanoparticles for UV/sunlight-driven degradation and antibacterial disinfection, Colloids Surf. A: Physicochem. Eng. Asp. 727 (2025) 138212, https://doi.org/10.1016/j.colsurfa.2025.138212.

[23] Y.-P. Liang, Y.-B. Chan, M. Aminuzzaman, M. Shahinuzzaman, S. Djearamane, K. Thiagarajah, S.-Y. Leong, L.-S. Wong, L.-H. Tey, Green synthesis and characterization of copper oxide nanoparticles from Durian (Durio Zibethinus) Husk for environmental applications, Catalysts 15 (3) (2025) 275, https://doi.org/10.3390/catal15030275.

[24] İ. Polat, S. Yılmaz, İ. Altın, E. Bacaksız, M. Sökmen, The influence of Cu-doping on structural, optical and photocatalytic properties of ZnO nanorods, Mater. Chem. Phys. 148 (3) (2014) 528–532, https://doi.org/10.1016/j.matchemphys.2014.07.011.

[25] I. Hasan, A. Bassi, P. Kalakonda, CuO surface functionalized β-cyclodextrin grafted PMMA hybrid nanocomposite for advance oxidative mineralization of methyl orange, Surf. Interfaces 56 (2025) 105456, https://doi.org/10.1016/j.surfin.2024.105456.

[26] I. Kir, H.A. Mohammed, S.E. Laouini, M. Souhaila, G.G. Hasan, J.A.A. Abdullah, S. Mokni, A. Naseef, A. Alsalme, A. Barhoum, Plant extract-mediated synthesis of CuO nanoparticles from lemon peel extract and their modification with polyethylene glycol for enhancing photocatalytic and antioxidant activities, J. Polym. Environ. 32 (2) (2024) 718–734, https://doi.org/10.1007/s10924-023-02976-x.

[27] V. Molahalli, A. Sharma, K. Bijapur, G. Soman, A. Shetty, B. Sirichandana, B.G. M. Patel, N. Chattham, G. Hegde, Properties, synthesis, and characterization of Cu-based nanomaterials, in: A. Srivastava, A. Srivastava (Eds.), ACS Symposium Series, ACS Symposium Series, 1466, American Chemical Society, Washington, DC, 2024, pp. 1–33, https://doi.org/10.1021/bk-2024-1466.ch001.

[28] Y.-K. Phang, M. Aminuzzaman, Md. Akhtaruzzaman, G. Muhammad, S. Ogawa, A. Watanabe, L.-H. Tey, Green synthesis and characterization of CuO nanoparticles derived from Papaya peel extract for the photocatalytic degradation of Palm oil mill effluent (POME), Sustainability 13 (2) (2021) 796, https://doi.org/10.3390/su13020796.

[29] P.P. Sarma, P. Borah, M.R. Das, P.K. Baruah, Agro-waste ash extracts facilitated green synthesis of CuO nanoparticles with efficient catalytic and photocatalytic activities for environmental remediation, J. Water Process Eng. 70 (2025) 107004, https://doi.org/10.1016/j.jwpe.2025.107004.

[30] V. Selvanathan, M. Aminuzzaman, L.-H. Tey, S.A. Razali, K. Althubeiti, H. I. Alkhammash, S.K. Guha, S. Ogawa, A. Watanabe, Md. Shahiduzzaman, Md. Akhtaruzzaman, Muntingia Calabura leaves mediated green synthesis of CuO nanorods: exploiting phytochemicals for unique morphology, Mater. (Basel) 14 (21) (2021) 6379, https://doi.org/10.3390/ma14216379.

[31] Y. Zhu, L. Huang, M. Liang, Z. Zhang, H. Xie, X. Sheng, X. Li, M. Zhong, B. Zhou, Green synthesis of plate-shaped CuONPs using Macleaya Cordata (Wild.) R.BR extracts for photocatalytic degradation and antibacterial properties, Biomass Conv. Bioref. 14 (22) (2024) 29175–29187, https://doi.org/10.1007/s13399-023-04943-x.

[32] J. Li, J.Z. Zhang, Optical properties and applications of hybrid semiconductor nanomaterials, Coord. Chem. Rev. 253 (23–24) (2009) 3015–3041, https://doi.org/10.1016/j.ccr.2009.07.017.

[33] P.A. Luque, A. Castro-Beltran, A.R. Vilchis-Nestor, M.A. Quevedo-Lopez, A. Olivas, Influence of pH on properties of ZnS thin films deposited on SiO2 substrate by chemical bath deposition, Mater. Lett. 140 (2015) 148–150, https://doi.org/10.1016/j.matlet.2014.10.167.

[34] N.S.N. Hasnan, N.A. Nordin, M.A. Mohamed, Synergistic Interaction and Hybrid Association of Conducting Polymer Photocatalysts/Photoelectrodes for emerging visible light active photocatalytic applications, J. Mater. Chem. A 12 (41) (2024) 27892–27931, https://doi.org/10.1039/D4TA03977G.

[35] N.K. Madipoju, S.J. Khanam, G. Sunkari, S.M. Vasamsetti, V. Divyasri, V. Morampudi, R.N. Savu, M. Banavoth, S. Banne, I. Hasan, P. Kalakonda, Bimetallic zinc-silver nanocomposites for superior antimicrobial efficacy, Appl. Phys. A 131 (2) (2025) 153, https://doi.org/10.1007/s00339-025-08289-1.

[36] S. Yano, R. Schroeder, B. Ullrich, H. Sakai, Absorption and photocurrent properties of thin ZnS films formed by pulsed-laser deposition on quartz, Thin. Solid. Films. 423 (2) (2003) 273–276, https://doi.org/10.1016/S0040-6090(02)01037-4.

[37] L.F.M.F. Cardozo, L.M. Pedruzzi, P. Stenvinkel, M.B. Stockler-Pinto, J.B. Daleprane, M. Leite, D. Mafra, Nutritional strategies to modulate inflammation and oxidative stress pathways via activation of the master antioxidant switch Nrf2, Biochimie 95 (8) (2013) 1525–1533, https://doi.org/10.1016/j.biochi.2013.04.012.

[38] S. Patil, M. Vedashree, P.S. Murthy, Valorization of coffee leaves as a potential agri-food resource: bio-active compounds, applications and future prospective, Planta 255 (3) (2022) 67, https://doi.org/10.1007/s00425-022-03846-x.

[39] K. Mehra, S. Kukreti, M. Kaushik, A comparative catalytic kinetics study for exploring dye degradation potential of silver, gold and palladium nanoparticles, J. NanoPart Res. 25 (7) (2023) 151, https://doi.org/10.1007/s11051-023-05795-2.

[40] A. Tabet, S. Meneceur, S.E. Laouini, C. Salmi, H.A. Mohammed, I. Kir, G.G. Hasan, F. Alharthi, J.A.A. Abdullah, One post biosynthesis of novel ternary nanocomposite ZnO/CuO/Cu2MgO3 for enhancing photocatalytic degradation of bromocresol green in wastewater, J. Clust. Sci. 35 (3) (2024) 765–777, https://doi.org/10.1007/s10876-023-02519-3.

[41] A. Serouti, L.S. Eddine, S. Meneceur, G.G. Hasan, H.A Mohammed, C. Salmi, K. Iman, M.F Ferhat, O.B. Ali, J.A. Abdullah, A. Biogenic ZnO/CuO/Fe2O3 nanocomposite: a groundbreaking approach for enhanced degradation capabilities and reusability in dye removal applications, Arab. J. Sci. Eng. 49 (1) (2024) 753–764, https://doi.org/10.1007/s13369-023-08495-0.

[42] K. Parvathalu, K. Rajitha, B. Chandrashekar, K. Sathvik, K. Pranay Bhasker, B. Sreenivas, M. Pritam, P. Pushpalatha, K. Moses, P. Bala Bhaskar, Biomimetic synthesis of copper nanoparticles using Tinospora Cordifolia plant leaf extract for photocatalytic activity applications, Plasmonics 19 (2) (2024) 825–834, https://doi.org/10.1007/s11468-023-02037-y.

[43] G. Sunkari, S. Vijaylaxmi, S. Lakshmi Mynepally, S.M. Vasamsetti, N.K. Madipoju, N.K. Dabbeta, P. Kumar, P.B. Kalakonda, L.C. Kalakonda, V. Morampudi, S. Jammalamadaka, P. Kalakonda, Synergistic antibacterial activity of green-synthesized Ag-Fe-Zn trimetallic nanocomposites using Tinospora Cordifolia leaf extract, Mater. Chem. Phys.: Sustain. Energy (2025) 100048, https://doi.org/10.1016/j.macse.2025.100048.

[44] U. Habib, F. Ahmad, M. Awais, N. Naz, M. Aslam, M. Urooj, A. Moqeem, H. Tahseen, A. Waqar, M. Sajid, M.J. Shabbir, Sustainable catalysis: navigating challenges and embracing opportunities for a greener future, JCE 2 (2) (2023) 14–53, https://doi.org/10.56946/jce.v2i2.205.

[45] A. Rafiq, M. Ikram, S. Ali, F. Niaz, M. Khan, Q. Khan, M. Maqbool, Photocatalytic degradation of dyes using semiconductor photocatalysts to clean industrial water pollution, J. Ind. Eng. Chem. 97 (2021) 111–128, https://doi.org/10.1016/j.jiec.2021.02.017.

[46] A. Atri, F. Dhaouadi, N. Mechi, L. Sellaoui, M. Echabaane, R. Ben Chaabane, A. Erto, M. Badawi, A. Ben Lamine, Removal of textile pollutants from aqueous medium using biosynthesized CuO nanoparticles: theoretical comparative investigation via analytical model, Heliyon. 10 (5) (2024) e26285, https://doi.org/10.1016/j.heliyon.2024.e26285.

[47] H. Akhter, S.S. Ritu, S. Siddique, F. Chowdhury, R.T. Chowdhury, S. Akhter, M. Hakim, *Silico* molecular docking and ADMET prediction of biogenic zinc oxide nanoparticles: characterization, and in vitro antimicrobial and photocatalytic activity, RSC Adv. 14 (49) (2024) 36209–36225, https://doi.org/10.1039/D4RA06890D.

[48] S. Pasieczna-Patkowska, M. Cichy, J. Flieger, Application of fourier transform infrared (FTIR) spectroscopy in characterization of green synthesized nanoparticles, Molecules 30 (3) (2025) 684, https://doi.org/10.3390/molecules30030684.

[49] T.M. El-Messery, E.A. Mwafy, A.M. Mostafa, H.M.F. El-Din, A. Mwafy, R. Amarowicz, B. Ozçelik, Spectroscopic studies of the interaction between isolated polyphenols from coffee and the milk proteins, Surf. Interfaces 20 (2020) 100558, https://doi.org/10.1016/j.surfin.2020.100558.

[50] J. Thyr, J. Montero, L. Österlund, T. Edvinsson, Energy alignment of quantum-confined ZnO particles with copper oxides for heterojunctions with improved photocatalytic performance, ACS Nanosci. Au 2 (2) (2022) 128–139, https://doi.org/10.1021/acsnanoscienceau.1c00040.

[51] Y.B. Chan, M. Aminuzzaman, L.-H. Tey, Y.F. Win, A. Watanabe, S. Djearamame, Md. Akhtaruzzaman, Impact of diverse parameters on the physicochemical characteristics of green-synthesized zinc oxide–Copper oxide nanocomposites derived from an aqueous extract of Garcinia Mangostana L, Leaf. Mater. (Basel) 16 (15) (2023) 5421, https://doi.org/10.3390/ma16155421.

[52] A.K.D. Alsukaibi, Various approaches for the detoxification of toxic dyes in wastewater, Processes 10 (10) (2022) 1968, https://doi.org/10.3390/pr10101968.

[53] C. Clavero, Plasmon-induced hot-electron generation at nanoparticle/metal-oxide interfaces for photovoltaic and photocatalytic devices, Nat. Photon 8 (2) (2014) 95–103, https://doi.org/10.1038/nphoton.2013.238.

[54] J. Yao, H. Wang, J. Fang, S. Shan, S.D. Joseph, L. Van Zwieten, K. Zhu, D. Chen, H. Jia, Distribution hotspots, formation mechanisms, and ecological effects of reactive oxygen species in soil and sediment: a critical review, Environ. Sci. Technol. 59 (27) (2025) 13551–13565, https://doi.org/10.1021/acs.est.5c00581.